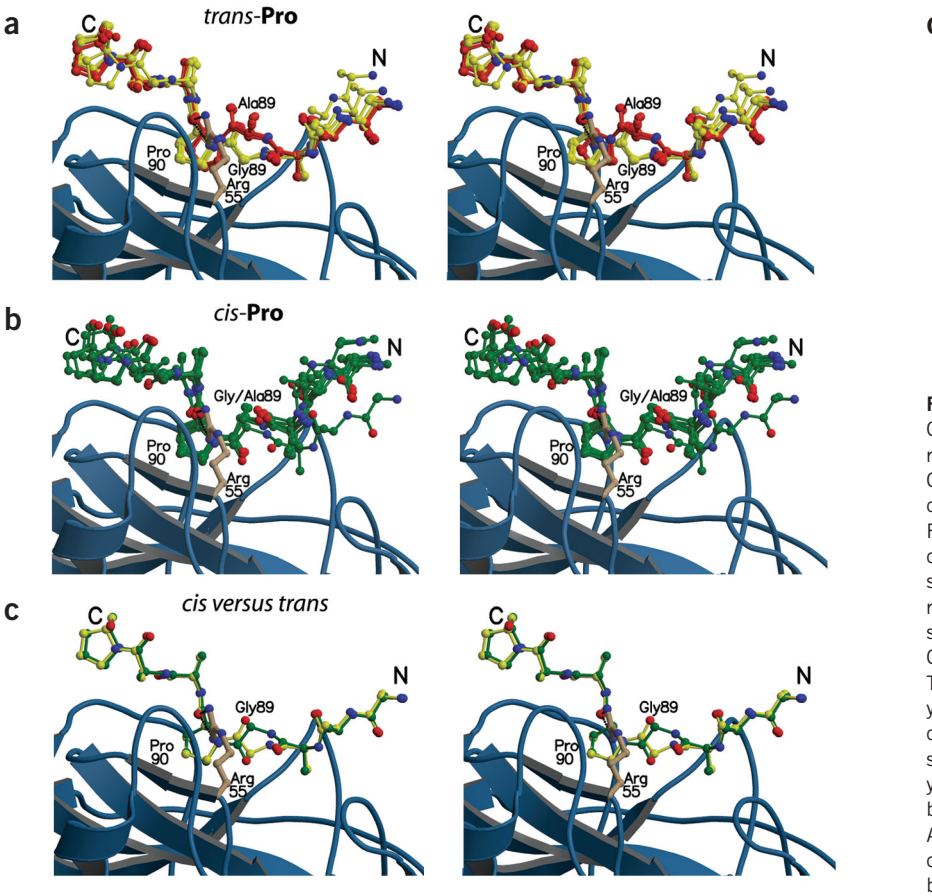

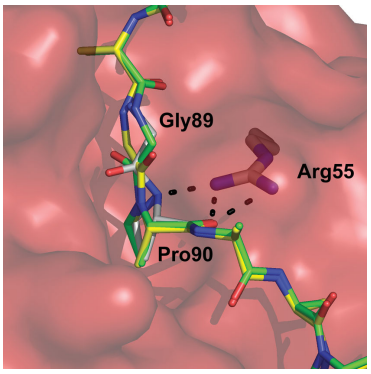

Figure 2 Comparison of CA^N loop conformations. CA^N residues 86–93 are shown as a stick representation with side chains truncated to the Cβ atom (except for proline) and carbon atoms colored yellow or orange (*trans*) and green (*cis*). For all figures, the minor (20% occupied) *cis* conformations of AMA-A and AMA-A′ are not shown unless explicitly stated. CypA is shown in a ribbon representation with the Arg55 side chain shown explicitly. (**a**) Stereo view showing all eight CA^N structures that adopt the *trans* conformation. The four structures that contain Gly89 are colored yellow; the four Ala89 structures are colored orange. (**b**) Same as **a** but for all eight *cis* CA^N structures. (**c**) Comparison of AAG-A (*trans*, yellow) and AMG-A (*cis*, green). (**d**) Same as **c**, but top view. CypA molecular surface colored red. A model for the transition state is shown with the carbon atoms colored white. Hydrogen bonds between CypA Arg55 and CA^N Pro90 N and O atoms are shown as dashed lines.

tion and include both *cis* and *trans* conformations. In one case, both conformations are seen in the same asymmetric unit with partial occupancy. The crystal structures support a mechanism in which substrate residues C-terminal to the isomeric proline remain stationary.

RESULTS

CypA–CA^N structures

We have refined crystal structures of the wild-type (WT) and five variant CA^N complexes with CypA that present views of 16 crystallographically independent complexes (**Table 1**) at resolutions of 1.7–2.0 Å and R_{free} of 22–26%. The crystals adopt space group $P2_1$ with two complexes in the asymmetric unit, except for two of the variants, which adopt space group $P1$ with four complexes in the asymmetric unit. The two crystal forms are very closely related: the $P1$ crystals differ from perfect $P2_1$ symmetry by rotation of <1° and translation of <0.5 Å between pseudo-equivalent molecules. The variants are named for their sequences (**Table 1**), and crystallographically independent structures are designated A or B for their position in the asymmetric unit, with the $P1$ crystals also containing A′ and B′ complexes.

Table 1. Constructs crystallized

	CA^N sequences (residues 82–97)	A[a]	B	A′	B′
WT(HAG)	-R L H P V H A G P I A P G Q M R-	*T*[b]	*T*		
AAG	-R L H P V **A** A G P I A P G Q M R-	*T*	*T*		
AMG	-R L H P V **A** **M** G P I A P G Q M R-	*C*	*C*		
AAA	-R L H P V **A** A **A** P I A P G Q M R-	*T*	*C*	*T*	*C*
AMA	-R L H P V **A** **M** **A** P I A P G Q M R-	*T*/*C*[c]	*C*	*T*/*C*[c]	*C*
O-loop	-R **T** H P **P** **A** **M** G P **L** **P** P G Q **I** R-	*C*	*C*		

[a]A, B, A′, B′ denote different CypA–CA^N complexes in the asymmetric unit. [b]*T, trans; C, cis.* [c]AMA-A and AMA(A′) are predominantly *trans* with a minor *cis* conformation.

The high-resolution structure of the M-type HIV-1_{NL43} CA^N–CypA complex is essentially identical to the medium-resolution structure reported earlier[17], with the central CA Gly89-Pro90 peptide in the *trans* conformation. In contrast, the chimeric O-loop CA^N construct, in which the CypA-binding loop was replaced by the O-type HIV-$1_{MVP5180}$ sequence, bound in the *cis* conformation (**Table 1**). To investigate this unexpected observation further, we made a series of chimeric loops in which O-type residues were substituted into the original M-type CA^N protein. This strategy allowed us to obtain single-residue variants that bind either in the *cis* or the *trans* conformation (**Table 1**).

In all structures reported here, the inherently flexible CypA-binding loop of CA (ref. 26) is ordered, with the central Pro90 residue adopting *B*-values that are comparable to those of surrounding residues in the CypA active site. The ensemble of structures includes cases in which both *cis*- and *trans*-Pro conformations occur in the same crystal lattice and even in equivalent asymmetric units (that is, as partial occupancy). This supports the assumption that the crystal structures represent on-pathway ground-state structures of the CypA-catalyzed isomerization. As expected from the database of known structures[27], all of the *cis*-Pro90 side chains adopt the *endo* pucker, whereas the *trans*-Pro90 side chains are found in both *endo* and *exo* puckers. Also as expected, the pucker of *trans*-Pro90 residues correlates with their ϕ angle; structures containing alanine at residue 89 have a relatively less negative ϕ angle and *exo* pucker, whereas the other *trans* structures